**MAPPING AND MODELING OF A TESSERA COLLISON ZONE, TELLUS REGIO, VENUS.** M. S. Gilmore[1], P. G. Resor[1], R. Ghent[2], D. A. Senske[3], R. R. Herrick[4] [1]Dept. of Earth and Environmental Sciences, Wesleyan University, Middletown CT, 06459, mgilmore@wesleyan.edu, [2]Univ. of Toronto, [3]JPL, [4]University of Alaska Fairbanks.

**Introduction:** Venus tessera terrain is characterized by two or more sets of intersecting structures that result in high radar backscatter [1,2]. Tessera terrain comprises ~8% of the Venus surface and occurs as large (1000s km across) plateaus (1-4 km above mean planetary radius) and small outcrops (<100 km across) at plains elevations [3]. The tesserae are generally embayed by plains materials, but yield crater ages of 1 – 1.4X the average surface age of the planet of ~800 Ma [1, 3-9]. Thus tesserae are the oldest materials on Venus and yield unique constraints on pre-plains geologic history and the plains forming event. Goals of this study are to perform high resolution (~100 m/pixel) mapping of a specific tessera highland, Tellus Regio, and determine the type, stratigraphy and wavelength of structures. These parameters are then input into a linearized model in order to estimate lithospheric properties of this highland through time.

**Geomorphic Mapping:** Tellus Regio is a plateau-shaped highland in the northern hemisphere of Venus that covers an area of ~$2x10^6 km^2$, making it the 3rd largest contiguous tessera highland on the planet. Previous analyses of Tellus [10-12] have identified a number of geomorphic units with distinct structural fabrics that we also recognize in this analysis of Magellan FMAP data. The oldest recognizable structures found in each unit are ridges, and units may contain several generations of ridges and graben. Four units are visible in the SW margin of Tellus, where a fold belt (Fig. 1, B) consisting of plains materials lies between 3 tessera units (Fig. 1, A, C, D). NW-trending ridges (and NE-trending graben) are recognized in the fold belt and adjacent tessera units (units A and C) and are attributed to contemporaneous compressional deformation. The NW- trending ridges differ morphologically from older fabrics preserved in the 3 regions of tessera terrain. These observations support the hypotheses that 1) tessera fabrics can form under distinct strain histories, and that 2) SW Tellus was formed by the assembly of these preexisting fabrics and intervening plains during a collisional event.

**Structural Wavelengths**: Ridge crests were identified by examining Cycle 1 and Cycle 3 left-looking image pairs and correlating these data to SAR characteristics typical of ridges (e.g., sinuous planform, gradual brightness changes across the ridge). Ridge wavelengths were computed in ArcGIS by measuring distances between nearest mapped ridge crests at 10s of

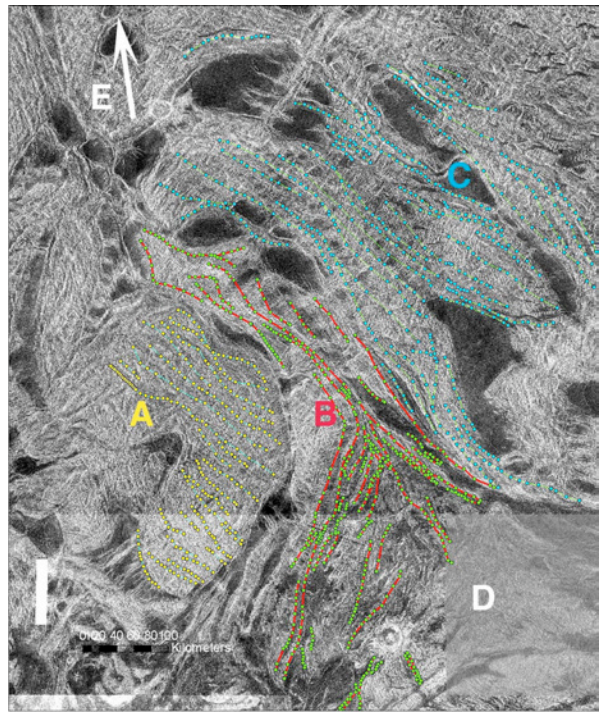


**Fig. 1. FMAP image of SW Tellus Regio. Lines indicate ridge crests used to measure structural wavelengths. A - "Indenter", B – Fold belt, C – Plateau interior, D – SE geomorphologic unit, E – to the western margin. Image subtends ~28-35°N, 75-81°E; north is up.**

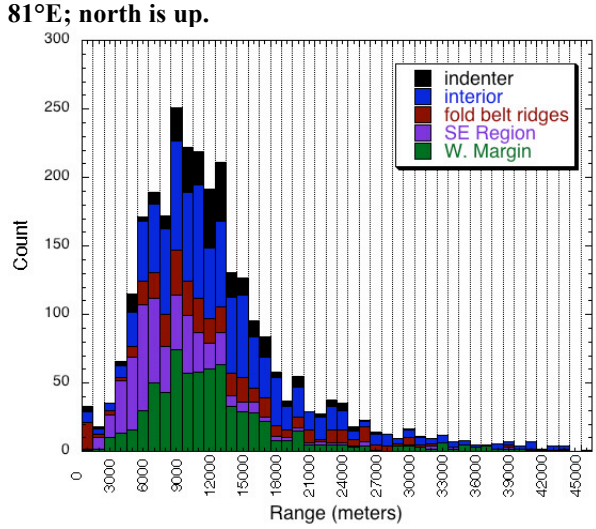


**Fig. 2. Histogram of ridge crest to crest distances in SW and western Tellus Regio (SE region includes trough to trough distances). Regions correspond to those in Fig 1.**

points along each ridge (dots in Fig. 1). Dominant wavelengths for mapped tessera regions are shown in Fig. 2.

Mean fold wavelengths of the tessera interior, indenter and western margin ~13 km (Fig. 1 C, A, E; Fig. 2). The wavelengths measured here are similar to those derived for the whole of Tellus Regio (n=23 measurements) and other tessera plateaus [13, 14].

Smaller mean wavelengths of ~ 8 km are recorded in the tessera of SE portion of Fig. 1 (area D) and for the materials of the fold belt (area B). Shortening estimates for the ridge belt were calculated by comparing the total length along a topographic profile to distance on the surface using topopgraphy generated from Magellan Cycle 1 and Cycle 3 left-looking stereopairs. A minimum shortening is derived by assuming that the plate is buckling with no internal deformation. This yields shortening values of <1%, similar to that reported for folds in Ovda Regio [15].

**Lithosphere Modeling:** To evaluate the lithospheric implications of fold wavelengths at Tellus Regio we have implemented the linearized perturbation model of [16] in Matlab® following the approach of [17]. In this model a single dominant wavelength instability develops in repsonse to layer-parallel strain of a relatively stiff brittle surface layer overlying a relatively soft ductile substrate [e.g., 18]. The thickness of the brittle layer and strength profile with depth of the ductile layer are dependent on composition, strain rate, and thermal gradient. We have taken a heuristic approach, forward modeling over likely ranges of thermal gradient and strain rate to find the range of values that yields the observed fold wavlengths. Strain rates were limited to the range of values estimated by [19]. Based on our low strain estimates (<1%) we have not adjusted the observed wavelengths for finite strain effects. All models used the dry Columbia diabase flow law of Mackwell et al. [20] (Table 1).

**Table 1. Thermal gradient (K/km) inferred from perturbation modeling.**

| Wavelength (km) | Strain rate ($s^{-1}$) $10^{-15}$ | $10^{-15.5}$ | $10^{-16}$ | Brittle layer thickness (km) |
|---|---|---|---|---|
| 8[1] | 73 | 66 | 59 | 2 |
| 13[2] | 38 | 33 | 29 | 3 |
| 20[3] | 21 | 19 | 17 | 5 |

[1]regions B and D (Fig. 1), [2]regions A and C, [3] conservative estimate [13]

**Discussion:** Systematic measurements of ridge wavelengths across SW Tellus Regio yield values that are similar over large portions of the area, consistent with similar lithospheric properties across this region. An exception to this is the folds and troughs of the tessera unit in the SE corner of Fig. 1, which records structures of a different wavelength and orientation than the remainder, implying a unique strain history or lithsopheic properties. The ridge belt also deforms at a shorter wavelength than the surrounding tessera regions. These plains materials are perhaps more likely to comprise thinner crust, or include detachment surfaces that allow shallow deformation at shorter wavelengths. NW-trending ridges (and NE-trending graben) across all units lie at the same stratigraphic level and are interpreted to result from a collisional event that deformed preexisting tessera and plains materials. Thus the formation of the oldest tessera fabric predates plateau formation. SW Tellus contains a clear example of the incorporation of plains materials into this tessera plateau and requires that plains formation was occurring contemporaneously with some stages of tessera plateau formation (uplift).

Modeling of folds using a minimum strain criterion yields thermal gradients of 29-73 K/km for the range of observed wavelengths and reasonable strain rates [19]. These values greatly exceed ~ 5 K/km estimates for the present-day near-surface thermal gradient [e.g., 21], and exceed the 17 K/km conservative model estimate of [13] that assumed 15 km wavelength folds and 25% strain. Strain estimates significantly less than 25% may be reasonable based on low amplitude to wavelength ratios (~1:10) of the folds in Tellus Regio. High thermal gradients and high surface temperatures may, however, permit significant distributed strain that is not reflected in the fold measurements. Surface-breaking thrust faults would also lead to unaccounted strain.

**References:** [1] Sukhanov (1992) in *Venus Geology, Geochemistry and Geophysics*, Univ. Ariz Press. [2] Barsukov et al. (1986) *JGR,* 91*,* D378. [3] Ivanov and Head (1996) *JGR 101*, 14861. [4] Bindschadler and Head (1991) *JGR* 96, 5889. [5] Bindschadler et al. (1992) *JGR* 97, 13563. [6] Solomon et al., (1992) *JGR*, 97, 13199. [7] Ivanov and Head (2001) *JGR* 106, 14515. [8] Ivanov and Basilevsky (1993) *GRL* 20, 2579. [9] McKinnon et al. (1997) in *Venus II*, Univ. Ariz Press. [10] Senske and Plaut (2000) *LPSC 31*, #1496. [11] Senske (1999) *LPSC 30,* #1668. [12] Straley and Gilmore (2007) *LPSC 38*, #1657. [13] Brown and Grimm (1997) *EPSL 147*, 1. [14] Ghent and Tibuleac (2002) *GRL 29*. [15] Ghent and Hansen (1999) *Icarus 139,* 116. [16] Fletcher and Hallet (1983) *JGR 88,* 7457. [17] Dombard and McKinnon (2001) *Icarus 154,* 321. [18] Biot (1961) *GSAB 72,* 1595. [19]Grimm (1994) *JGR 99*, 23163. [20] Mackwell et al. (1998) *JGR 103,* 12053. [21] Smrekar and Parmentier (1996) *JGR 101*, 5397.

**Acknowledgement:** Support from NASA PG&G is gratefully acknowledged. Thanks to Max Gardner for help with digitizing and GIS work.